NUMERICAL STUDY OF NONLINEARITY OF UNSTEADY AERODYNAMICS FOR NLR-7301 PROFILE

Kenichi Saitoh[1], Ralph Voss[2] and Hamidreza Kheirandish [3]

[1] Institute of Space Technology and Aeronautics, Japan Aerospace Exploration Agency
6-13-1, Osawa, Mitaka-shi, Tokyo 181-0015, Japan
email: saitoh.kenichi@jaxa.jp

[2] Institute of Aeroelasticity, German Aerospace Center
Bunsenstrasse 10, 37073 Goettingen, Germany
email: Ralph.Voss@dlr.de

[3] Research Center of Computational Mechanics, Inc.
1-7-1, Togoshi, Shinagawa-ku, Tokyo 142-0041, Japan
email: hamid@rccm.co.jp

Key words: Unsteady aerodynamics, Limit cycle oscillation, Transonic flutter

Abstract. Details of unsteady aerodynamics for two dimensional wing of NLR-7301 with flap were numerically investigated by Navier-Stokes code in transonic regime. Unsteady aerodynamic coefficients such as lift and pitching moment show non-linear aspects in small amplitude range of forced excitation mode. Pressure distribution of super sonic region on upper surface is very sensitive to the incidence and this brings the nonlinearity of the unsteady aerodynamics in small amplitude range of pitching motion. Behavior of re-attachment of the boundary layer aft of shock wave also affects the nonlinearity. Shock wave motions were also examined. Linearized unsteady lift and pitching moment coefficients for each amplitude were applied to the eigen value analysis for the flutter boundary. Flutter simulations were also carried out and the results showed that the amplitude of the limit cycle oscillation could be explained by the flutter boundary of the eigen value analysis.

1 INTRODUCTION

To synthesize a control law for an aero-servo-elastic system, a state equation is required first. It is, for example, expressed by an equation of motion for an elastic system with external aerodynamic force. As far as subsonic flow is considered, linear expression is available for aerodynamics and static deflection and amplitude of oscillation has no significant role.

As for the symmetric wing profile, Davis and Malcom[1] experimentally showed the linearity

of the unsteady lift coefficient for NACA 64A010 profile at Mach 0.80 up to one deg. of amplitude in pitching motion. In this case there is no strong shock wave which generate shock induced flow separation. Using the small disturbance code, Isogai[2] also showed that the unsteady coefficients of lift and pitching moment were linear in pitching motion up to amplitude of 0.5 deg. and 0.2 deg. at Mach 0.80 and 0.85 respectively for the same wing profile. It is said it is linear as far as there is no strong shock wave to generate major flow separation. These results mean the unsteady aerodynamics in transonic flow can be expressed by the linearized aerodynamics coefficients if there is no major flow separation. On the other hand, Bendiksen[3] showed the nonlinearity of static lift and pitching moment around zero degree of incidence by the Euler analysis for NACA00 series profile. This means it is nonlinear even with the small amplitude at least in quasi-steady condition.

Supercritical wing profile which is "shock free" at design condition has been investigated, especially for NLR-7301 profile by Tijdeman[4] et al. Recently two dimensional flutter experiment has been carried out in DLR and interesting results such as Limit cycle oscillation (LCO) were observed[5]. In this paper it is described about the results of unsteady aerodynamics and LCO simulations for two dimensional wing of NLR-7301 with flap investigated by the numerical analysis with Navier-Stokes code.

2 COMPUTAION CODE

2.1 Code

Computation code which is used in this paper is developed by Kheirandish, based on the following method.

Equation	Thin layer 2D Navier-Stokes Equation
Turbulence model	Boldwin-Lomax
Differential method	implicit TVD scheme
Integral method	ADI scheme
Structural solver	Willson's implicit θ method
Grid system	Structured C type

A module for flap rotation mode was added to the original code. Flap rotates at the center in wing thickness direction without gap. Hinge position is at 75% chord for all calculation. Grids for 0 and 8 deg. flap deflection are shown in Fig.1. Although there is no special arrangement at the hinge point, there is no grid broken. It is defined that downward rotation at trailing edge is positive for the flap deflection. The grid size is 261（203 on wing）×71. The minimum grid space which is normalized by half chord length is $2x10^{-4}$in normal direction to the wing, and 0.025 in tangential direction. Reynolds number is $1x10^{6}$ except for the code validation

calculation. The transition point is automatically calculated and the flow is supposed laminar when the turbulent viscosity satisfies $\mu_{tur} \leq 14$.

2.2 Unsteady analysis

To evaluate the unsteady aerodynamics, sinusoidal forced excitation was given as

$$x(\tau) = x_0 + \bar{x}\sin(k\tau) \qquad (1)$$

where x is a deflection or displacement of the mode, x_0 is its mean value, $\bar{x}$ is an amplitude, k is a reduced frequency and $\tau = tU/b$ is a nondimensional time. Unsteady aerodynamic coefficient y, which is a time history obtained by a simulation, is expressed in a Fourier series as

$$y(\tau) = \frac{1}{2}y_0 + \bar{x}\sum_m \left\{ y_{R,m}\sin(mk\tau) + y_{I,m}\cos(mk\tau) \right\} \qquad (2)$$

Although the nonlinearity appears in higher harmonic components, the second order components of C_l is 1.5% of the first order's one for the pitching mode with 0.5 deg. amplitude and k=0.20 at Mach 0.750. Each simulations have five periods and 8,000 time steps per one period for the cases of the reduced frequency is more than or equal to 0.20. The time step size $\Delta\tau$ =0.004 at k=0.20. Lower than k=0.20, time steps were used more than 8,000 to avoid large time step size.

2.3 Validation

A calculated result was compared with the experimental results of AGARD test case[7]. The flow condition is Mach 0.70, 2.0 deg incidence and Re=1.07x10^6. In this condition, the shock wave exist around 40%c. Fig.2 shows the unsteady pressure distribution for flap oscillation with k=0.71 and amplitude of 1.0 deg. The shock wave of the calculated result is aft compared with the experimental result and the phase seems to be delayed.

3 COMPUTATIONAL RESULTS

3.1 Steady results

Steady C_p distributions are shown in Fig.5 to 8. At Mach 0.750 shock wave stays at the same location even when the incidence changes, where at Mach 0.700 it moves aft as the incidence increases. The shock wave location is defined where supersonic flow decelerates to be a sonic speed on the wing, even for a "shock free" condition. As for the flap deflection, the shock moves aft as the deflection increases even at Mach 0.750.

C_p distribution in local supersonic region on the upper surface is very sensitive to the incidence between -0.4 and +0.1 deg. at Mach 0.750 (Fig.10). The C_p distribution in supersonic region sinks at the center if the incidence is lower than -0.1 deg. The skin frictions also show changes of flow pattern as shown in Fig.9. The boundary layer separated at the shock wave is re-attached in downstream with the incidence between -0.4 deg. and +0.1 deg. But the re-attachment does not appear at -0.2 deg., at which the flat part of the C_p distribution in the supersonic region sinks a little. These re-attachments of the flow separation are corresponding to the unsteady pressure distributions as described later.

3.2 Unsteady results

Unsteady lift and pitching moment coefficient are shown in Fig.11 and 12. In the figures, the first harmonic components of the Fourier series are plotted in its magnitude and phase. The pitching moment is evaluated at 25% chord position. The mean angle of attack in the unsteady calculations is -0.2 deg., at which a singularity is observed in the steady results. The unsteady coefficients in the figures are normalized by the amplitude of the excitation mode, so those are constant according to the amplitude, if those are linear to the amplitude. Nonlinearity of unsteady C_m is clearer than of C_l. Those variations are observed not only in the large amplitude but also very small amplitude. Peaks of unsteady pressure distributions are at 20%c and 60%c in Fig.13. With the small amplitude, the variations are seen at 20%c and between 30 and 40%c in local supersonic region. At the shock wave position, the variations are small. With larger amplitude, the shock wave propagates from aft to the front and appears again at rear position. The peaks of the unsteady pressure distribution become small and the distributions become flat with large amplitude.

The difference in unsteady pressure distribution at 65-70%c can be seen between 0.3 and 0.4 deg. amplitude in Fig.13. Unsteady C_f distribution around this area shows more clear difference. With the amplitude more than 0.2 deg., reattachment of the boundary layer separation appears in the aft area of shock wave in Fig.14.

The shock waves travel distance corresponding to the amplitude of the pitching motion is shown in Fig.15. Except 0.3 and 0.4 deg. amplitude, the traveling distance is proportional to the pitching amplitude. Effect of the reduced frequency of pitching motion on the shock wave travel distance is shown in Fig.16. As it is observed that the shock wave does not move at Mach 0.750 in steady condition even if the incidence is changed, the shock wave travel distance is small in lower reduced frequency than 0.20.

Unsteady pressure distributions for the flap mode are the same in smaller amplitude than 0.4 deg. and the peak at the shock becomes lower with more amplitude as shown in Fig.19. With

0.5deg. amplitude the unsteady pressure distributions change from 0.4 deg. amplitude and the re-attachment of the flow separation appears. It is different from the pitching mode that the shock wave moves in low reduced frequency in Fig.21.

3.3 Flutter/LCO analysis

The unsteady coefficients of lift and pitching moment are linearized and applied to the p-k method for a flutter analysis. Experimental model carried out in DLR was used for structural model[5]. The flutter boundary is obtained according to the amplitude of the pitching mode. (Fig. 22). Flow condition is Mach 0.750 and mean angle of attack is -0.2 deg. For the amplitude ratio $\Delta\alpha/(\Delta h/b)$, 1.3 is used which is the results observed in the simulation. The unsteady coefficients are calculated for the reduced frequency of 0.10 and 0.15 and interpolated, while the reduced frequency in the LCOs are 0.122. The boundary is constant between 0.5 and 2.0 deg. of pitching amplitude, and it is "stabilized" beyond 2.0 deg. It is also stabilized in the amplitude smaller than 0.5 deg. LCO simulations were conducted to evaluate the boundary. By the p-k analysis the amplitude of the pitching mode in the LCO is estimated 3.0 and 2.7 deg. for F_i=0.20 and 0.18 respectively. The results of the LCO simulations show that the amplitude is 3.2 and 3.0 deg. respectively and those are reasonable compared with the p-k analysis. When the initial values of α, h, $\dot{\alpha}$ and $\dot{h}$ are zero, the deviation from the equivalent condition becomes an initial disturbance because the simulation starts from the steady results in fixed condition. In this case the response converges as shown in Fig.25 at F_i=0.17. In the case that the initial values are $\dot{\alpha}$ =0.317 and $\dot{h}$ =0.00728, the response got into the LCO condition and it means the initial condition determines the stability of the response. Although the boundary also insists on the existence of the LCO with small amplitude, it has not been observed in the simulation.

4 CONCLUDING REMARKS

The numerical analysis with Navier-Stokes code shows the unsteady transonic aerodynamics has nonlinear characteristics in very small amplitude for the NLR-7301 super critical wing. Re-attachment of the flow separation enlarges the nonlinearity. But flutter analysis based on the eigen value analysis with linearlized unsteady aerodynamics gives a insight of LCO condition. It is thought that a linear controller for aero-servo-elastic system in transonic region can be synthesized with considering the nonlinearity caused by the amplitude of vibration mode as a system error.

5 REFERENCES

[1] S. S. Davis, G. W. Malcom, “Experiments in Unsteady Transonic Flow”, AIAA 79-0769, 17th Aerospace Sciences Meeting, New Orleans, La., 1979

[2] K. Isogai, “Numerical Study of Transonic Flutter of a Two-Dimensional Airfoil”, NAL TR 617T, 1980

[3] O. O. Bendiksen, “Improved Similarity Rules for Transonic Flutter”, AIAA 99-1350

[4] H. Tijdeman, “Investigations of the transonic flow around oscillating airfoils”, NLR TR 77090U, 1977

[5] G. Schewe, H. Mai, G. Dietz, “Nonlinear Effects in Transonic Flutter with Emphasis on Manifestations of Limit Cycle Oscillations”, Journal of Fluids and Structures Vol. 18, Issue 1 , August 2003, P 3-22

[6] H. Kheirandish, et al., “Numerical Flutter Simulation of a Binary System in Transonic Region”, Aircraft Symposium, Hiroshima, Japan, 1995

[7] U. R. Mueller, H. Henke, “Computation of Transonic Steady and Unsteady Flow about the NLR 7301 Airfoil”, Notes on Numerical Fluid Mechanics, Vol.5x, 1996

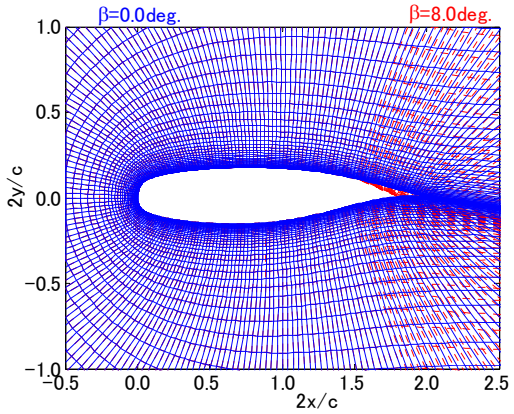

Fig.1 Grid (β=0.0 & 8.0 deg.)

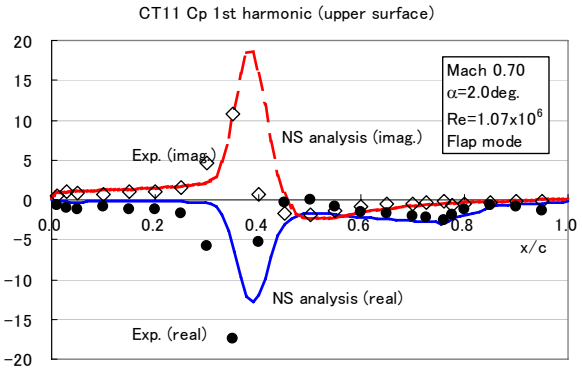

Fig.2 Unsteady pressure distribution for flap mode (Mach 0.70, α=2.0deg, k=0.071, Δβ=1.0deg, Re=1.07x10^6)

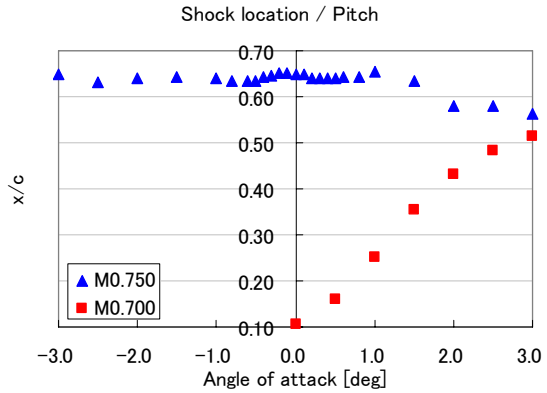

Fig.3 Steady shock wave location (pitching)

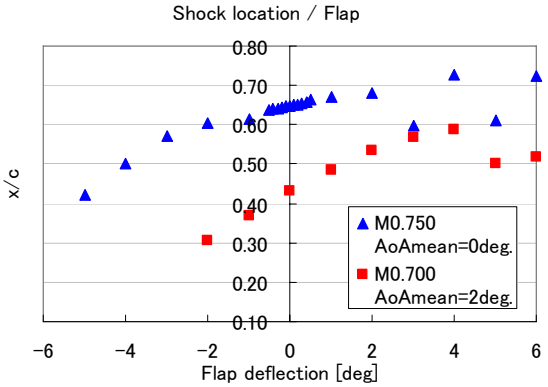

Fig.4 Steady shock wave location (flap)

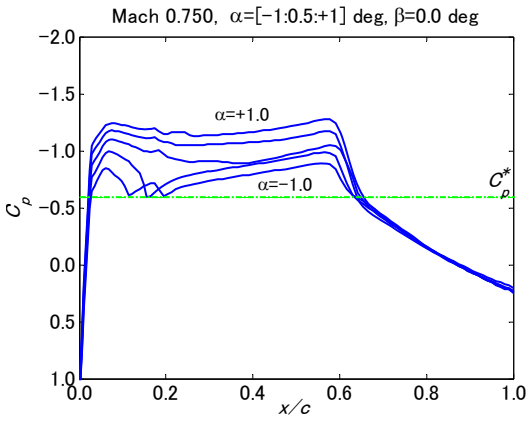

Fig. 5 Steady pressure disributions (α=-1 to +1deg.)

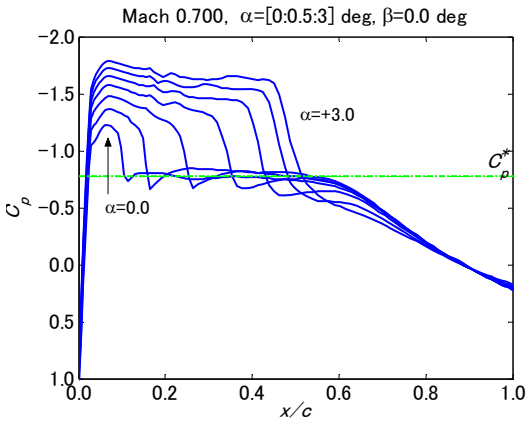

Fig. 6 Steady pressure disributions (α=0 to +3deg.)

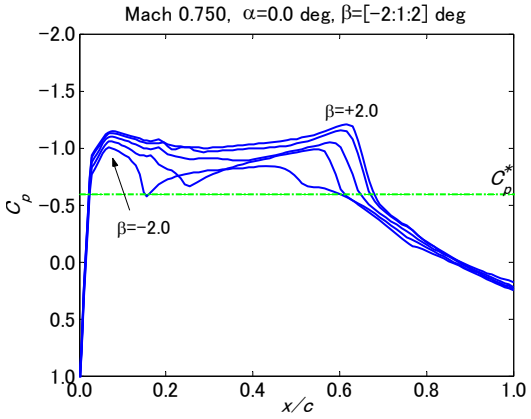

Fig.7 Steady pressure disributions (β=-2 to +2deg.)

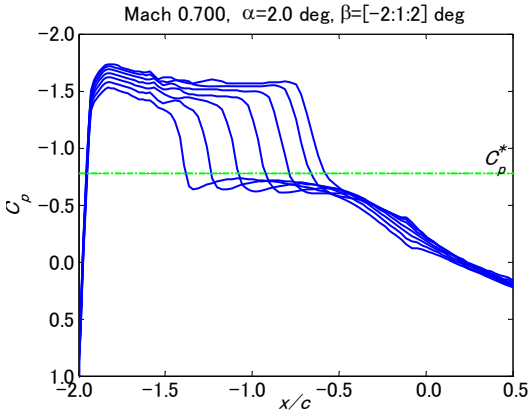

Fig. 8 Steady pressure disributions (β=-2 to +2deg.)

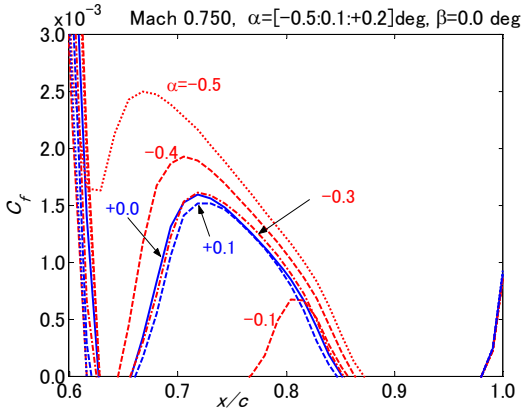

Fig. 9 Steady skin friction distributions

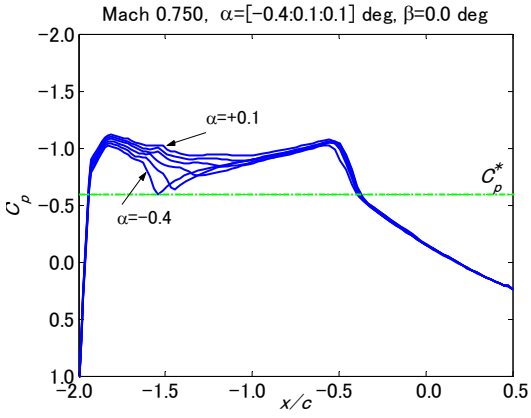

Fig. 10 Steady pressure disributions (α=-0.4 to +0.1deg.)

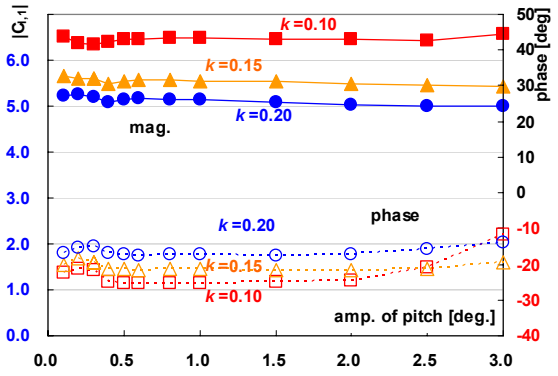

Fig.11 Unsteady C_l for pitch motion (first harmonic component)

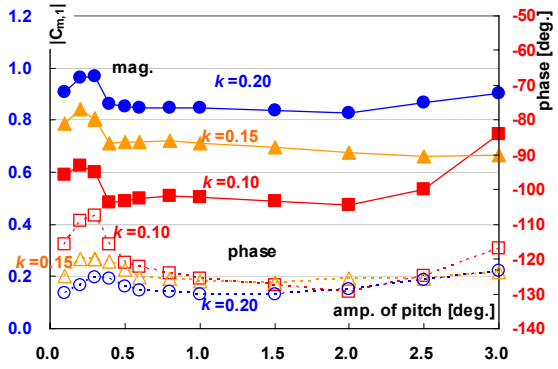

Fig.12 Unsteady C_m for pitch motion (first harmonic component)

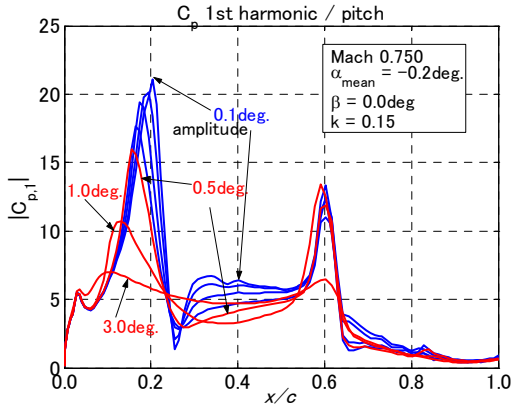

Fig.13 Unsteady pressure distributions for pitching motion

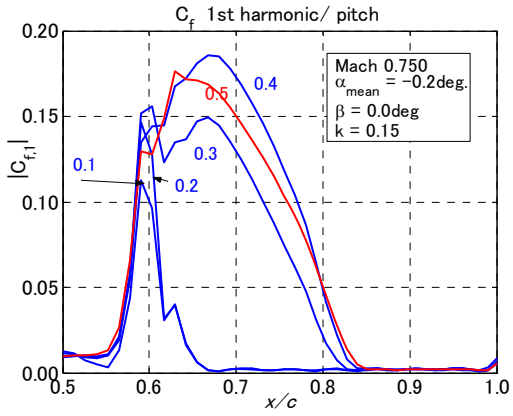

Fig.14 Unsteady skin friction distributions for pitching motion

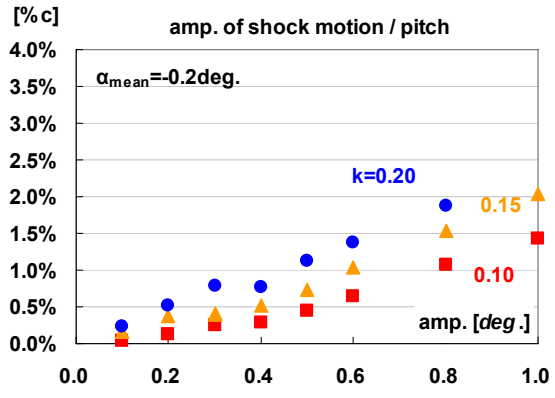

Fig.15 Shock traveling distance for pitching mode

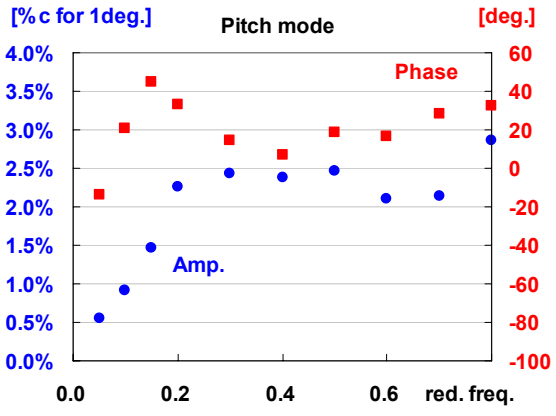

Fig.16 Frequency response of shock motion for pitch (Δα=0.5deg.)

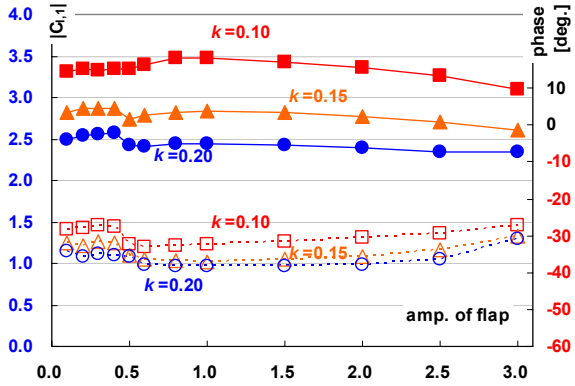

Fig.17 Unsteady C_l for flap motion (first harmonic component)

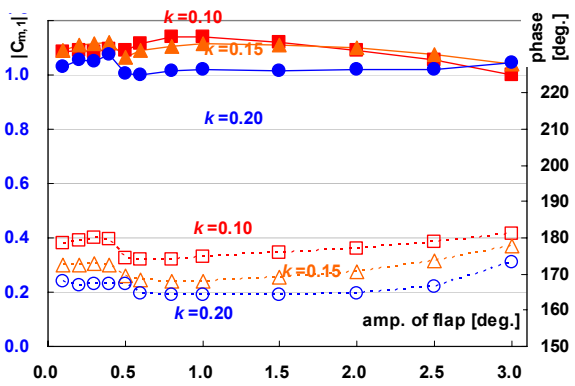

Fig.18 Unsteady C_m for flap motion (first harmonic component)

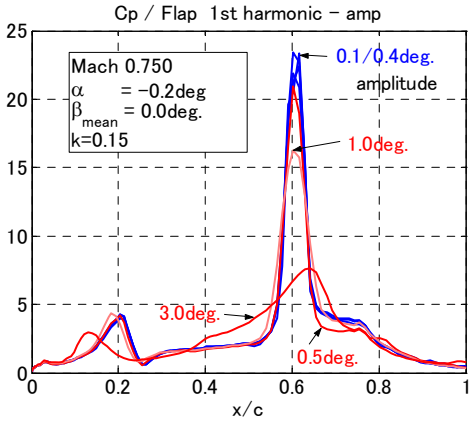

Fig.19 Unsteady pressure distributions for flap motion

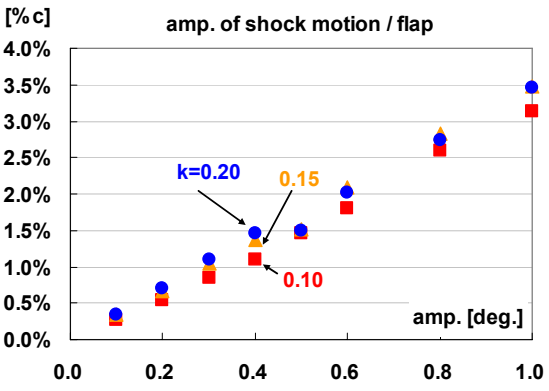

Fig.20 Shock traveling distance for flap mode

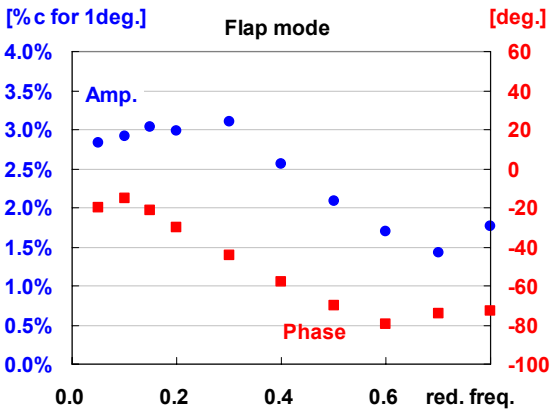

Fig.21 Frequency response of shock motion for flap (Δβ=0.5deg.)

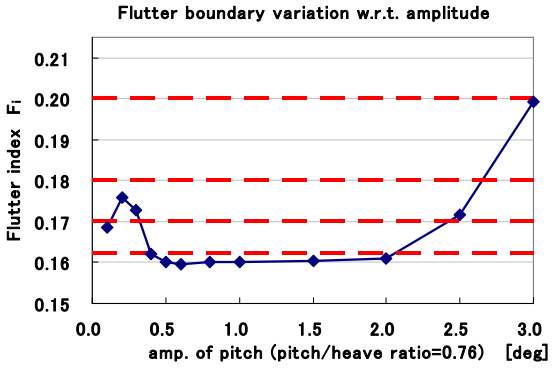

Fig.22 Flutter boundary by eigen value analysis

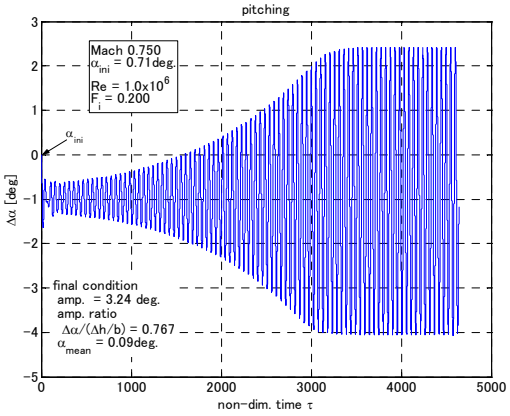

Fig.23 Time history of pitching (F_i=0.200)

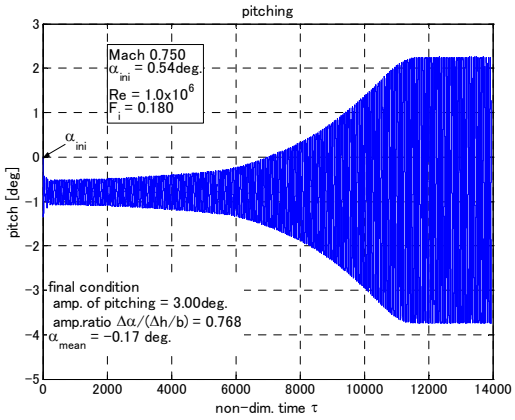

Fig.24 Time history of pitching (F_i=0.180)

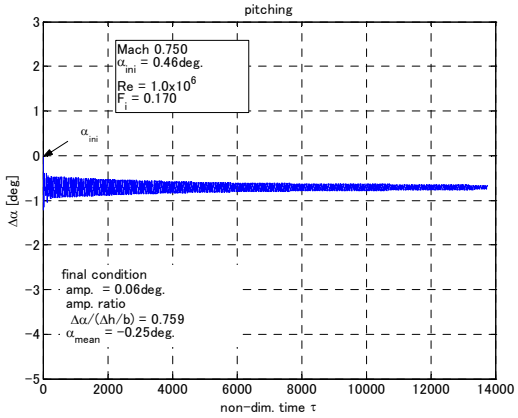

Fig.25 Time history of pitching (F_i=0.170)

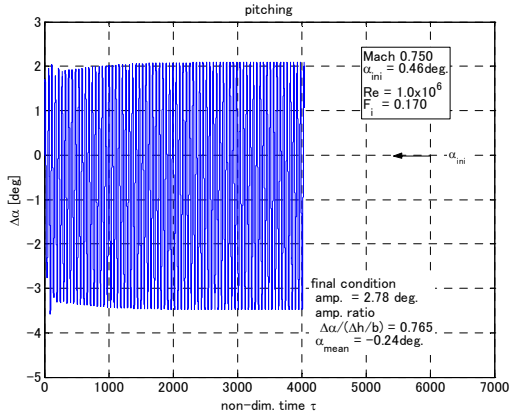

Fig.26 Time history of pitching (F_i=0.170)

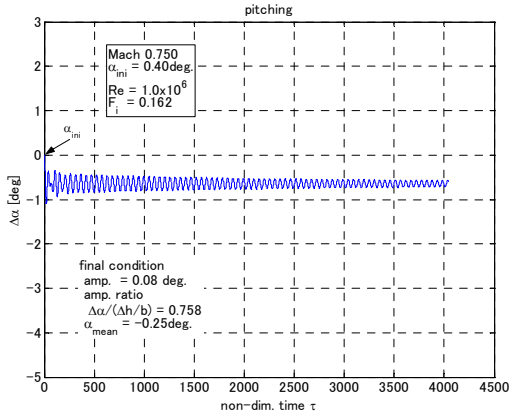

Fig.27 Time history of pitching (F_i=0.162)